Wavelet-Galerkin Scheme of Inhomogeneous Electromagnetic Problems in the Time Domain

정영욱* · 이용민** · 최진일*** · 나극환*** · 강준길*** · 신철재****

Young-Wook Cheong* · Yong-Min Lee** · Jin-Il Choi*** · Keuk-Hwan Ra***
· Joon-Gil Kang*** · Chull-Chai Shin****

요 약

본 논문은 시변 맥스웰 방정식에 기초한 웨이브릿-갤러킨 설계를 제안하였다. 두 개의 모멘트 함수가 0 이 되는 Daubechies 웨이브릿 함수를 기저함수로 전개하고 Yee가 제안한 Leap-frog 접근법을 적용하였다. Daubechies 웨이브릿의 변위된 보간 특성을 이용하여 적분이나 매체 연산자에 대한 부가적인 행렬이 필요없는 방정식을 유도하였다. 안정화 조건을 유도하고 분산특성을 분석한 후 유한차분 시간영역법과 다해상도 시간영역법의 결과와 비교하였고, 분산특성의 분석을 통해 기저함수의 정규성(Regularity)과 받침폭(Support width) 사이의 균형을 확인했다. 기저함수가 단 2개의 0이 되는 웨이브릿 모멘트 함수를 가지지만, 이는 수치해석 상에서 무시할 수 있는 분산 오류를 수반하였고, 컴팩트 받침(Compact support)에 의해 노드 당 적은 수의 계수만이 고려되었다. 제안된 설계의 저장계수의 효율, 실행 시간의 감소와 정확도를 균일 공진기와 비균일 공진기의 공진주파수 해석을 통해 검증하였다.

Abstract

A wavelet-Galerkin scheme based on the time-dependent Maxwell's equations is presented. Daubechies' wavelet with two vanishing wavelet moments is expanded for basis function in spatial domain and Yee's leap-frog approach is applied. The shifted interpolation property of Daubechies' wavelet family leads to the simplified formulations for inhomogeneous media without the additional matrices for the integral or material operator. The stability condition is formulated. The dispersion characteristics are analyzed and compared with those of finite difference time domain and multiresolution time domain methods. The analyses show the excellent trade-off between the regularity and the support width of the basis function. Although the basis function has only two vanishing wavelet moments, it is enough to provide negligible dispersive error in the numerical analysis and its compact support enables only several involved terms per nodes. The storage effectiveness, execution time reduction and accuracy of this scheme are demonstrated by calculating the resonant frequencies of the homogeneous and inhomogeneous cavities.

* 에이스테크놀로지 통신기술연구소(Communication R&D Institute, Ace Technology)
** 한국과학기술연구원 복합기능 세라믹 연구센터(Division of Ceramics, KIST)
*** 광운대학교 전자공학과(Dept. of Elec., Kwangwoon Univ.)
**** 아주대학교 전자공학과(Dept. of Elec., Ajou Univ.)
· 논 문 번 호 : 990222-019
· 수정완료일자 : 1999년 4월 24일

I. Introduction

Recently, methods employing numerical analysis based on wavelet to investigate the wave propagation characteristics of structures have attracted the attention of many researchers. Among them, the multiresolution time domain (MRTD) method[1] shows an excellent capability to approximate the exact solution even for near Nyquist sampling limit while the traditional Yee algorithm[2] needs 10 or more grid points per wavelength.

In the MRTD scheme, however, integral equations have to be evaluated for inhomogeneous media[1]. Moreover, when the required data are sampled and source is applied, many terms of the field components are considered[1],[3]. This is due to the nonlocalization characteristics of the cubic spline Battle-Lemarie wavelet function. As an alternative basis, compactly supported wavelet is possible to make the considered terms reduced. For the inhomogeneous electromagnetic problem, wavelet-Galerkin (WG) method with compactly supported Daubechies' wavelet was derived by M. Werthen and I. Wolff[4]. Their approach need not the integral equations but the operator of the material distribution and a few terms of the field components are considered in sampling and source embedding. However, it has two disadvantages. At first, in contrast to MRTD and finite difference time domain (FDTD) schemes, the unknown field components are redundant because the BCR coefficients[5] are directly used. The second disadvantage is that the additional operator still exists for the calculation of the material distribution. To overcome these drawbacks, the derivative filter coefficients need to be revcalculated at integer and half translation and a simple sampling technique should be applied.

In this paper, both transient and Fourier concerns are formulated from the inner product of scaling function and its first-order derivative. And the shifted interpolating property of Daubechies' wavelet family[6] is adopted to achieve the pure and simple sampling procedure.

This scheme is tested with the trial function of Daubechies' tap-4 wavelet in single channel approach. Maxwell's curl equations are formulated through Galerkin procedure. Related dispersion characteristics are derived and compared with FDTD and MRTD correspondents. And then the numerical experiments in a homogeneous and three inhomogeneous resonant structures are implemented and compared with those of FDTD. These results show that WG scheme based on leap-frog and shifted interpolating techniques is very feasible for the inhomogeneous electromagnetic scattering problems.

II. Theory

A multiresolution analysis of $L^2(\mathbf{R})$ is defined as a sequence of closed subspaces V_j of $L^2(\mathbf{R})$, $j \in \mathbf{Z}$, with the following properties[7]:

1. $V_j \subset V_{j+1}$,
2. $f(x) \in V_j \Leftrightarrow f(2x) \in V_{j+1}$,
3. $f(x) \in V_0 \Leftrightarrow f(x+1) \in V_0$,
4. $\bigcup_{j=-\infty}^{+\infty} V_j$ is dense in $L^2(\mathbf{R})$ and $\bigcap_{j=-\infty}^{+\infty} V_j = \{0\}$,
5. There exists a scaling function $\varphi \in V_0$,

with a nonvanishing integral, such that $\{\varphi(x-k)\}_{k\in Z}$ is a Riesz basis of V_0.

As an orthogonal complement of V_j in V_{j+1}, the subspaces W_j are defined as

$$V_{j+1} = V_j \oplus W_j \tag{1}$$

and the space $L^2(\mathbf{R})$ is represented as a direct sum,

$$L^2(\mathbf{R}) = \bigoplus_{j\in Z} W_j. \tag{2}$$

Since $\varphi \in V_0 \subset V_1$, a sequence $h_k \in l^2(\mathbf{Z})$ exist such that the scaling function satisfies

$$\varphi(x) = 2\sum_k h_k \varphi(2x-k). \tag{3}$$

This recursive equation is fundamental to the theory of the scaling function and referred to by several different names: the refinement equation, the dilation equation, the multiresolution analysis equation, or the two-scale difference equation. The collection of functions $\{\varphi_{j,k} \mid j, k \in \mathbf{Z}\}$, with $\varphi_{j,k}(x) = 2^{j/2}\varphi(2^j x-k)$, is a Riesz basis of V_j.

Similarly, a wavelet function is defined such that the set of functions $\{\psi_{j,k} \mid j, k \in \mathbf{Z}\}$, with $\psi_{j,k}(x) = 2^{j/2}\psi(2^j x-k)$ is a Riesz basis of W_j. Since the wavelet ψ is an element of V_1, a sequence $g_k \in l^2(\mathbf{Z})$ exists such that

$$\psi(x) = 2\sum_k g_k \varphi(2x-k). \tag{4}$$

Suppose we consider only finite scale expansions in terms of scaling or wavelet functions which is what happens in practice. If we let for fixed scale $j = 0$,

$$\tilde{f}(x) = \sum_k c_{0,k}\,\varphi_{0,k}(x), \tag{5}$$

then $\tilde{f}$ is a wavelet interpolation of original function $f(x)$ at the subspace V_0. From (1), we can reexpress $\tilde{f}$ in terms of scaling and wavelet functions at coarser scales,

$$\tilde{f}(x) = \sum_k c_{0,k}\varphi_{0,k}(x) = \sum_k c_{j_0,k}\varphi_{j_0,k}(x) + \sum_k \sum_{j=j_0}^{0} d_{j,k}\psi_{j,k}(x) \quad \text{for } j_0 < 0. \tag{6}$$

The wavelet representation of a sampled function of the form (5) allows one to use the scaling functions at a given scale as finite element or Galerkin-type basis functions in a discrete approximation to some continuous problems[8]. The multiscale representation of data is also available as given in (6) to implement multigrid iterative schemes for solving hyperbolic boundary problems[1],[4],[9]. There are some algorithms needed for partial wavelet embedding in terms of an adaptive grid scheme. Without such scheme, there is a considerable increase of execution time, which is due to the interactions between the fine and coarse scales such as $V_j \rightarrow W_j$, $W_j \rightarrow V_j$ or $W_j \rightarrow W_j$[5]. In order to reduce the interactive terms and related coefficients, thresholding algorithm is generally applied[4],[9]. It results in the reduced execution time in the calculation of total nodes. On the other hand, this scheme leads to the increase in the complexity of a given method and takes an additional time to determine thresholding criteria.

We will take single channel scheme only with scaling functions at an adequately fine scale. Instead of the loss of the facet of multiresolution analysis and its adaptive gridding property, all routines are simplified and maintained in a unique form, and simple interpolation scheme is

usable. If one may choose the Daubechies' wavelet as a trial function in single channel, then its shifted interpolating property makes it possible to sample data per unit node without the additional integral[1] or material operator[4] in inhomogeneous or anisotropic media. Furthermore, the complete equations with the conductivity term are straightforward and similar to FDTD formulae. The multi-channel scheme or multiresolution approach will be introduced in Appendix.

Let us derive the WG scheme of Maxwell's curl equations using Daubechies' compactly supported wavelets[10].

Maxwell's curl equations in the time domain

$$-\mu\frac{\partial\vec{H}}{\partial t}=\nabla\times\vec{E}, \tag{7}$$

$$\sigma\vec{E}+\varepsilon\frac{\partial\vec{E}}{\partial t}=\nabla\times\vec{H} \tag{8}$$

may be approximated with various scaling functions. For examples, in the case of MRTD scheme, the field components are represented by a series of Haar scaling functions in time and cubic spline Battle-Lemarie bases in space, while in FDTD a series of Haar scaling functions is expanded in both time and space domain. For the generality of WG scheme, we define $h(t)$ as the Haar scaling function for time domain expansion and $\varphi(x)$ as the ortho normal scaling function for space, respectively.

The six components of electromagnetic field are expanded in terms of the tensor product of scaling functions

$$H_x(\vec{r},t)=\sum_{i,j,k,n=-\infty}^{+\infty}H^{\varphi x}_{i,j+1/2,k+1/2,n}\,\varphi_i(x)\cdot\varphi_{j+1/2}(y)\,\varphi_{k+1/2}(z)\,h_n(t), \tag{9}$$

$$H_y(\vec{r},t)=\sum_{i,j,k,n=-\infty}^{+\infty}H^{\varphi y}_{i+1/2,j,k+1/2,n}\,\varphi_{i+1/2}\cdot(x)\,\varphi_j(y)\,\varphi_{k+1/2}(z)\,h_n(t), \tag{10}$$

$$H_z(\vec{r},t)=\sum_{i,j,k,n=-\infty}^{+\infty}H^{\varphi z}_{i+1/2,j+1/2,k,n}\,\varphi_{i+1/2}\cdot(x)\,\varphi_{j+1/2}(y)\,\varphi_k(z)\,h_n(t), \tag{11}$$

$$E_x(\vec{r},t)=\sum_{i,j,k,n=-\infty}^{+\infty}E^{\varphi x}_{i+1/2,j,k,n-1/2}\,\varphi_{i+1/2}\cdot(x)\,\varphi_j(y)\,\varphi_k(z)\,h_{n-1/2}(t), \tag{12}$$

$$E_y(\vec{r},t)=\sum_{i,j,k,n=-\infty}^{+\infty}E^{\varphi y}_{i,j+1/2,k,n-1/2}\,\varphi_i(x)\cdot\varphi_{j+1/2}(y)\,\varphi_k(z)\,h_{n-1/2}(t), \tag{13}$$

$$E_z(\vec{r},t)=\sum_{i,j,k,n=-\infty}^{+\infty}E^{\varphi z}_{i,j,k+1/2,n-1/2}\,\varphi_i(x)\cdot\varphi_j(y)\,\varphi_{k+1/2}(z)\,h_{n-1/2}(t) \tag{14}$$

where $E^{\varphi x}_{i,j,k,n}$ and $H^{\varphi x}_{i,j,k,n}$ with $x=x,y,z$ are expansion coefficients in terms of scaling functions. Integers i,j,k and n indicate the discrete lattice indices in space and time grids related to the space and time coordinates via $x=i\Delta x$, $y=j\Delta y$, $z=k\Delta z$ and $t=n\Delta t$, where Δx, Δy, Δz and Δt represent the space discretization interval in x-, y-, z-direction and the time discretization interval, respectively.

The indices follow the traditional Yee's leap-frog scheme[2]. This provides a conditional stability for hyperbolic partial differential equation and the stability condition is typically of a form similar to the Courant stability condition for the general leap-frog method.

The $h_n(t)$ and $\varphi_i(x)$ functions are generated from the basic scaling functions by scaling and translation:

$$h_n(t)=h\left(\frac{t}{\Delta t}-n+\frac{1}{2}\right), \tag{15}$$

$$\varphi_i(x)=\varphi\left(\frac{x}{\Delta x}-i\right). \tag{16}$$

The Haar scaling function $h(t)$ is defined as

$$h(t)=\begin{cases}1 & \text{if } 0<t<1\\ 0 & \text{otherwise.}\end{cases} \tag{17}$$

The scaling functions are generally created from the product formula

$$\hat{\varphi}(\xi)=\prod_{j=1}^{\infty} H(2^{-j}\xi) \tag{18}$$

where $H(\xi)=\sum_k h_k e^{-ik\xi}$ and $\hat{\varphi}$ is the Fourier transform of φ defined as

$$\hat{\varphi}(\xi)=\int_{-\infty}^{+\infty}\varphi(x)\, e^{-i\xi x}dx. \tag{19}$$

Daubechies' scaling function $\varphi(x)$ with two vanishing wavelet moments (DB2) and its coefficients h_k are shown in Fig. 1 and Table I, respectively. The number of vanishing wavelet moments is denoted by p and given by

$$\int_{-\infty}^{+\infty} x^k \psi(x)\,dx \approx 0 \quad \text{for } 0\le k\le p-1,$$
$$k\in Z. \tag{20}$$

The property of wavelets with vanishing moments are important in approximation of smooth functions and operators.

The field expansions (9) to (14) are inserted in Maxwell's equations (7) and (8), and sampled using basis functions as test functions according to Galerkin method. For the sampling with respect to time in terms of Haar scaling function, the related inner products become

$$\langle h_n(t),\ h_{n'}(t)\rangle=\delta_{n,n'}\Delta t, \tag{21}$$

$$\langle h_{n-1/2}(t),\ \frac{\partial h_{n'}(t)}{\partial t}\rangle=\delta_{n,n'}-\delta_{n,n'+1} \tag{22}$$

where the inner product of two functions f, g is defined as

$$\langle f(x),\ g(x)\rangle=\int_{-\infty}^{+\infty} f(x)\,\overline{g(x)}\,dx \tag{23}$$

and $\delta_{n,n'}$ is the kronecker delta given by

$$\delta_{n,n'}=\begin{cases}1 & \text{for } n=n'\\ 0 & \text{for } n\neq n'.\end{cases} \tag{24}$$

In sampling with respect to an orthogonal lattice, the related integrals are obtained as

$$\langle \varphi_i(x),\ \varphi_{i'}(x)\rangle=\delta_{i,i'}\Delta x, \tag{25}$$

$$\langle \varphi_i(x),\ \frac{d}{dx}\varphi_{i'+1/2}(x)\rangle=\sum_l r(l)\,\delta_{i+l,i'}. \tag{26}$$

The coefficients $r(l)$ are calculated by these correspondents in time and frequency domain:

$$r(l)=\int_{-\infty}^{+\infty}\varphi(x+l)\frac{d}{dx}\varphi(x-\frac{1}{2})\,dx$$
$$=\frac{1}{2\pi}\int_{-\infty}^{+\infty} j\xi\,|\hat{\varphi}(\xi)|^2 e^{-j(l+\frac{1}{2})\xi}d\xi. \tag{27}$$

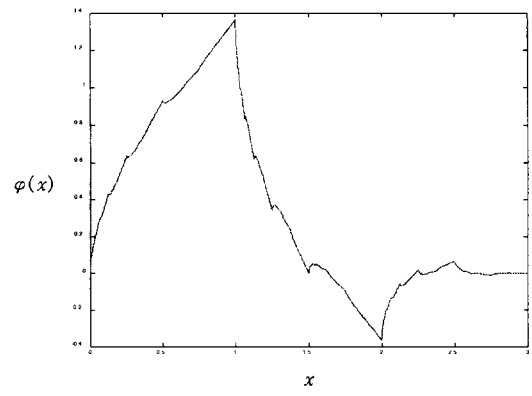

Fig. 1. Daubechies' scaling function with two vanishing wavelet moments.

Table 1. The coefficients h_k.

k	h_k
0	0.34150635094622
1	0.59150635094587
2	0.15849364905378
3	-0.09150635094587

Table 2. The coefficients $r(l)$.

l	$r(l)$
0	1.22916661202745
1	-0.09374997764764
2	0.01041666418309

For DB2, the coefficients $r(l)$ for $0 \le l \le 2$ are shown in Table II and for $l > 2$ are zeros due to the compact support of Daubechies' scaling function. The coefficients $r(l)$ for $l < 0$ are given by the symmetry relation $r(-1-l) = -r(l)$.

In Daubechies' scaling functions, the shifted interpolation property is almost satisfied. This property is given by the following lemma[6]:

Lemma 1 *If* $\varphi(\tau + k) = \delta_{k,0}$ with $k \in Z$ and $p \ge 1$, then $\tau = M_1$

where M_1 is the first order moment of the scaling function given by

$$M_1 = \int_{-\infty}^{+\infty} x\,\varphi(x)\,dx \tag{28}$$

and p is the number of vanishing wavelet moments.

Proof. Refer to [6].

To make use of the shifted interpolation property, (16) is modified to

$$\varphi_i(x) = \varphi\left(\frac{x}{\Delta x} - i + M_1\right). \tag{29}$$

For DB2, $M_1 = 0.6343975$. In spite of its support [0, 3], single point sampling of total field can be taken at integer points with negligible error. For example, E_x component at spatial point $((i+1/2)\Delta x, j\Delta y, k\Delta z)$ and at time $(n-1/2)\Delta t$ becomes

$$\begin{aligned} &E_x((i+1/2)\Delta x, j\Delta y, k\Delta z, (n-1/2)\Delta t) \\ &= \int\int\int\int E_x(\vec{r}, t)\,\delta\left(\frac{x}{\Delta x} - i - \frac{1}{2}\right) \\ &\cdot \delta\left(\frac{y}{\Delta y} - j\right)\delta\left(\frac{z}{\Delta z} - k\right)\delta\left(\frac{t}{\Delta t} - \frac{n+1}{2}\right) \\ &\cdot dx\,dy\,dz\,dt = E^{\varphi x}_{i+1/2,j,k,n-1/2} \end{aligned} \tag{30}$$

where δ is the Dirac delta function. It is noted that the sampled values are very dependent on the test function.

Using (21), (22), (25), (26) and (29), we obtain the scalar equations related to H_x and E_x corresponding to Maxwell's curl equations (10), (11):

$$\begin{aligned} &\frac{\mu_{i,i+1/2,k+1/2}}{\Delta t}\left(H^{\varphi x}_{i,j+1/2,k+1/2,n} - H^{\varphi x}_{i,j+1/2,k+1/2,n-1}\right) \\ &= \sum_l r(l)\left(\frac{E^{\varphi y}_{i,j+1/2,k+l+1,n-1/2}}{\Delta z}\right. \\ &\left. - \frac{E^{\varphi z}_{i,j+l+1,k+1/2,n-1/2}}{\Delta y}\right), \end{aligned} \tag{31}$$

$$\begin{aligned} &\frac{\sigma_{i+1/2,j,k}}{2}\left(E^{\varphi x}_{i+1/2,j,k,n+1/2} + E^{\varphi x}_{i+1/2,j,k,n-1/2}\right) \\ &+ \frac{\varepsilon_{i+1/2,j,k}}{\Delta t}\left(E^{\varphi x}_{i+1/2,j,k,n+1/2} - E^{\varphi x}_{i+1/2,j,k,n-1/2}\right) \\ &= \sum_l r(l)\left(\frac{H^{\varphi z}_{i+1/2,j+l+1/2,k,n}}{\Delta y}\right. \end{aligned}$$

$$-\frac{H^{\varphi y}_{i+1/2,j,k+1+1/2,n}}{\Delta z}\Big) \tag{32}$$

where $\mu_{i,j,k}$, $\sigma_{i,j,k}$ and $\varepsilon_{i,j,k}$ represent permeability, conductivity and permittivity at spatial point $(i\Delta x, j\Delta y, k\Delta z)$, respectively, and these quantities are measured by the formula

$$f_{i,j,k}=\int\int\int f(x,y,z)\,\delta\left(\frac{x}{\Delta x}-i\right)\delta\left(\frac{y}{\Delta y}-j\right)\cdot\delta\left(\frac{z}{\Delta z}-k\right)dx\,dy\,dz. \tag{33}$$

Other equations of electromagnetic field are obtained straightforwardly by the similar way.

Ⅲ. Stability Criteria

The stability condition of the WG scheme is derived by the similar way to those of FDTD[11] and MRTD with the scaling functions only (S-MRTD)[12]. For the WG scheme with DB2 (WG-DB2), the stability condition becomes

$$c\Delta t \le \frac{1}{\sum_{i=0}^{\pm 2}|r(i)|\sqrt{\frac{1}{(\Delta x)^2}+\frac{1}{(\Delta y)^2}+\frac{1}{(\Delta z)^2}}} = \frac{1}{\frac{4}{3}\sqrt{\frac{1}{(\Delta x)^2}+\frac{1}{(\Delta y)^2}+\frac{1}{(\Delta z)^2}}}. \tag{34}$$

Especially, for the scale $\Delta x=\Delta y=\Delta z=\Delta$, the stability condition becomes

$$c\Delta t \le 0.433013\Delta. \tag{35}$$

Ⅳ. Dispersion Analyses

In order to analyze the numerical dispersion of the WG-DB2 scheme, plane monochromatic traveling-wave modes are substituted into the discretized Maxwell's equations. For simplicity, the compact vector notation for Maxwell's equations is used for derivation[11].

For a normalized region of space with no loss, $\mu=1$, $\varepsilon=1$, we obtain

$$\left[\frac{1}{c\Delta t}\sin\left(\frac{\omega\Delta t}{2}\right)\right]^2 = \left[\frac{1}{\Delta x}\sum_{l_1=0}^{\pm 2} r(l_1)\sin\left\{\left(l_1+\frac{1}{2}\right)\tilde{k}_x\Delta x\right\}\right]^2 + \left[\frac{1}{\Delta y}\sum_{l_2=0}^{\pm 2} r(l_2)\sin\left\{\left(l_2+\frac{1}{2}\right)\tilde{k}_y\Delta y\right\}\right]^2 + \left[\frac{1}{\Delta z}\sum_{l_3=0}^{\pm 2} r(l_3)\sin\left\{\left(l_3+\frac{1}{2}\right)\tilde{k}_z\Delta z\right\}\right]^2. \tag{36}$$

To quantitatively assess the numerical dispersion characteristics of the WG scheme, we assume grids with equidistance in spatial do main ($\Delta x=\Delta y=\Delta z=\Delta$) and wave propagation at angles α and β. α denotes the angle bet ween x-axis and the propagation in the $z=0$ plane while β represents the angle between z-axis and propagation. Then numerical dispersion relation of (36) simplifies to

$$\left(\frac{\Delta}{c\Delta t}\right)^2\sin^2\left(\frac{\omega\Delta t}{2}\right) = \left[\sum_{l_1=0}^{\pm 2} r(l_1)\sin\left\{\left(l_1+\frac{1}{2}\right)\tilde{k}\cos\alpha\sin\beta\cdot\Delta\right\}\right]^2 + \left[\sum_{l_2=0}^{\pm 2} r(l_2)\sin\left\{\left(l_2+\frac{1}{2}\right)\tilde{k}\sin\alpha\sin\beta\cdot\Delta\right\}\right]^2 + \left[\sum_{l_3=0}^{\pm 2} r(l_3)\sin\left\{\left(l_3+\frac{1}{2}\right)\tilde{k}\cos\beta\cdot\Delta\right\}\right]^2. \tag{37}$$

(37) can be solved for the numerical wave vector $\tilde{k}$ at any wave propagation angle α and β by applying the iterative procedure of Newton's method:

$$\tilde{k}_{i+1} = \tilde{k}_i - \frac{f(\tilde{k}_i)}{f'(\tilde{k}_i)} . \tag{38}$$

The normalization of Δ to the free-space wavelength λ_0 is equivalent to normalizing the free-space wavelength to one unit. Then an initial guess for $\tilde{k}_0$ may be simply 2π, the wavenumber of the corresponding mode in free space. For this case, it is shown that the numerical phase velocity $\tilde{v}_p$ is given by

$$\frac{\tilde{v}_p}{c} = \frac{2\pi}{\tilde{k}_{\text{final}}} \tag{39}$$

where $\tilde{k}_{\text{final}}$ is the final result of the Newton's method iterations.

The calculated dispersion characteristics of the WG-DB2 scheme are shown in Fig. 2. While the numerical phase velocity of FDTD method is always slower than that of ideal case, the phase velocity in the WG-DB2 scheme fluctuates between faster and slower areas. In the FDTD method, the basis function in spatial domain has poor regularity because the number of its vanishing wavelet moment is one. Actually, 10 or more grids in the smallest wavelength is recommended in the FDTD discretization. DB2 has more regularity according to its two vanishing wavelet moments.

In the wavelets of Daubechies' family and other wavelet system, the more regularity can be obtained by increasing the number of filter coefficients or the degrees of freedom. The increase in the number of filter coefficients, however, leads to the heavy calculational burden. This is related to the support width of the basis function in Daubechies' family which has compact support. In case of wavelet with the infinite support such as Battle-Lemarie cubic spline wavelet, the truncated support width has relations with computational complexity. One can take tradeoff between the regularity and the support width.

Fig. 3 shows the dispersion characteristics of

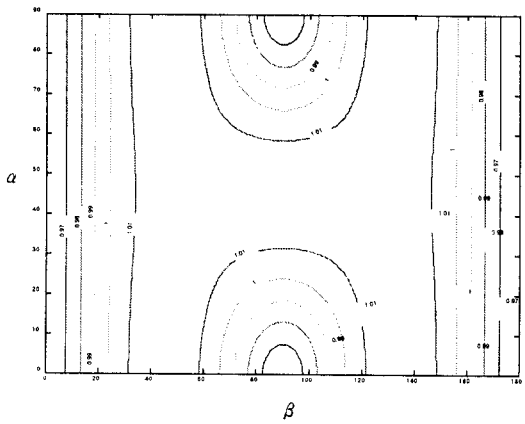

Fig. 2. Variation of the numerical phase velocity with wave propagation angles α and β in three dimensional WG-DB2 scheme ($\Delta = 0.4\,\lambda_0$ in spatial domain, $\Delta t = 0.1\Delta$ in time domain).

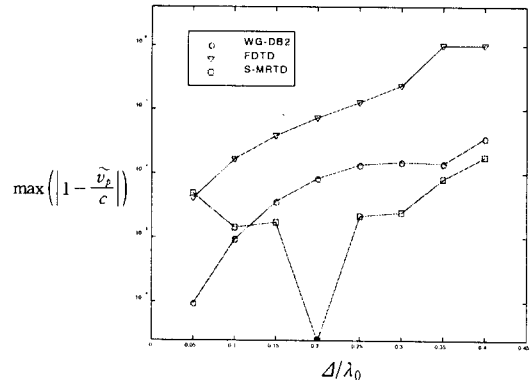

Fig. 3. Numerical dispersion characteristics of WG-DB2, FDTD, S-MRTD schemes according to various spatial discrete sizes (The time discretization is fixed as $\Delta t = 0.1\Delta$. Markers represent calculated points. The lines between markers are linearly interpolated.)

three different schemes with various spatial discrete sizes. The time discretization is fixed as $\Delta t = 0.1\Delta$. As described above, Δ/λ_0 smaller than 0.1 is recommended in FDTD. Discretization with $\Delta/\lambda_0 \gg 0.1$ leads to non-negligible error and the numerical cutoff grid level exists between 0.3 and 0.4. In WG-DB2 and S-MRTD, however, coarse grid level retains small error even at near Nyquist limit.

V. Numerical Results

To validate the current approach, numerical results for homogeneous and inhomogeneous rectangular cavities have been tested. The geometries of the tested cavities are shown in Fig. 4. In order to use a pulse excitation at $(i_0\Delta x,\ j_0\Delta y,\ k_0\Delta z, n_0\Delta t)$ with respect to space and time, the pulse in WG-DB2 is decomposed as

$$E^{\varphi x}_{i,j,k,n} = E^{\varphi x}_{i,j,k,n} + E^{pulse}_{i_0,j_0,k_0,n_0}\,\delta_{i,i_0}\,\delta_{j,j_0}\,\delta_{k,k_0}\,\delta_{n,n_0} \tag{40}$$

The frequency response can be obtained by the fast Fourier transform (FFT) at the specific points.

The compact support width longer than 1 leads to the additional embedding of tangential field components for modeling the boundary condition on the perfect electric conductor (PEC) or perfect magnetic conductor (PMC). According to the image principle, perfect electric or magnetic walls are modeled utilizing the symmetry conditions for the tangential fields. In particular, the electric and magnetic field components tangential to the PEC must have

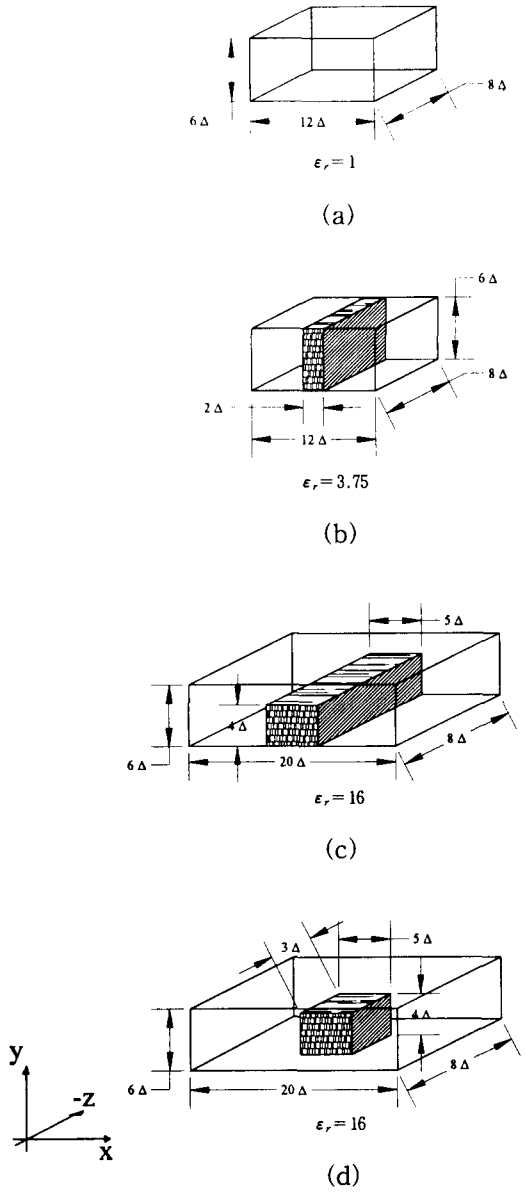

Fig. 4. Three dimensional homogeneous and inhomogeneous cavities.

odd and even symmetry, respectively. In the similar way, the perfect magnetic wall may be modeled by implanting even tangential electric fields and odd tangential magnetic fields with respect to the PMC.

The results are obtained with two different mesh sizes for WG-DB2 scheme and compared with the responses of FDTD with the fine mesh. All the numerical experiments are implemented with the same time discretization, $\Delta t = 10^{-9}\Delta$ and each procedure is iterative in 50,000 time step in order to obtain the steady-state solution. The results of WG-DB2 scheme show the good agreement with the analytic value and those of FDTD.

Table 3 summarizes the numerical results in terms of the normalized lowest resonant frequency, mesh size and execution time[1]. Compared with the conventional FDTD method, WG-DB2 scheme with coarse grid provided a 32:1 reduction in the required mesh size and a 13.4:1 reduction in the execution time for the air-filled cavity. In the inhomogeneous cavities, the reduction of the mesh size is limited to the geometries of the scattering objects. If the scatterer has a complex shape, the fine mesh must be used to eliminate the ambiguity in construction of geometry and the error related to the abrupt change of the material parameters such as permittivity, permeability and conductivity.

Especially in the dimension with the invariant or smoothly variant parameters, the coarse grid is still available. Table 3 supports this effect in the reduced computational burden.

About 1.7 times increase in computation time is observed in WG-DB2 scheme with the same grid discretization of FDTD method. However, WG-DB2 scheme provides more precise solution for the wide frequency range because of its relatively linear numerical dispersion even at near Nyquist sampling limit as shown in Fig. 2 and 3.

Table 3. Normalized lowest resonant frequencies for the cavities shown in Fig. 4

Cavities	Finite difference time domain			Wavelet-Galerkin with DB2			Analytic value
	Normalized resonant frequency	Mesh size	Execution time(sec)	Normalized resonant frequency	Mesh size	Execution time(sec)	
Cavity I Fig. 4 (a)	0.07473	12×6×8	54.9	0.07513	12×6×8	101.2	0.07512
				0.07593	3×3×2	4.1	
Cavity II Fig. 4 (b)	0.05227	12×6×8	59.4	0.05273	12×6×8	102.8	-
				0.05313	12×3×2	12.5	
Cavity III Fig. 4 (c)	0.02633	20×6×8	104.6	0.02660	20×6×8	175.8	-
				0.02633	8×3×2	8.9	
Cavity IV Fig. 4 (d)	0.03753	20×6×8	104.8	0.03813	20×6×8	175.9	-
				0.03793	8×3×8	34.2	

[1] The source program was written in C and executed using the IBM compatible PC with Pentium CPU. The execution time was measured in preprocessing and main procedures. The processes of FFT and visualization were not included in the execution time.

VI. Conclusion

The WG-DB2 scheme with shifted interpolation property has been derived. The simple interpolating approach allows the simplified form of equations for inhomogeneous media without the integral or material operator. The dispersion characteristics of the WG-DB2 scheme are analyzed and compared with those of other methods, FDTD and S-MRTD. It is shown that WG-DB2 provides the nearly linear numerical dispersion even around Nyquist limit.

The derived algorithm is tested in the numerical analyses of the homogeneous and inhomogeneous cavities. The results of the WG-DB2 scheme show the good agreement with the FDTD correspondents. For the homogeneous cavity the economy of computational storage and execution time in the WG-DB2 scheme with coarse grid is 32 times and 13.4 times greater than in the FDTD method, respectively, while its algorithm also retains the good accuracy of a numerical approximation. For the inhomogeneous media, the reduction of the mesh size is limited by its geometric complexity. The coarse grid is still available in the dimension with the smoothly variant parameters.

The derived scheme shows the excellent trade-off between the regularity and the support width of the basis function. Although the DB2 has only two vanishing wavelet moments, it provides small dispersive error in the numerical analyses and its narrow support enables several involved terms per node. Moreover, the shifted interpolation property of the Daubechies' wavelet family eliminates the additional matrix for the integral or material operator. It leads to the further reduction in the storage burden and the execution time.

Appendix

Extension to multiresolution scheme

For time and space adaptive gridding, wavelets as well as scaling functions are scaled and translated. In two-channel scheme in z-axis, the basis function of H_x is extended as

$$H_x(\vec{r}, t) = \sum_{i,j,k,n=-\infty}^{+\infty} \left(H^{\varphi x}_{i,j+1/2,k+1/2,n} \varphi_{k+1/2}(z) + H^{\psi x}_{i,j+1/2,k+1/2,n} \psi_{k+1/2}(z) \right) \cdot \varphi_{j+1/2}(y)\, \varphi_i(x)\, h_n(t) . \quad (41)$$

The wavelet function $\psi_i(x)$ is given by

$$\psi_i(x) = \psi\left(\frac{x}{\Delta x} - i + M_1\right) \quad (42)$$

where M_1 is the first order moment of the scaling function given by (28). The shift factor M_1 is also utilized for the multi-channel approach in Daubechies' wavelet family. The shifted interpolation property makes it possible to obtain single sampling per nodes in the region with the negligible wavelet coefficients.

In sampling with respect to an orthogonal lattice and orthonormal bases, the related integrals are obtained as (25), (26),

$$\langle \psi_i(x), \psi_{i'}(x) \rangle = \delta_{i,i'} \Delta x, \quad (43)$$

$$\langle \varphi_i(x), \psi_{i'}(x) \rangle = \langle \psi_i(x), \varphi_{i'}(x) \rangle = 0, \quad (44)$$

$$\langle \psi_i(x), \frac{d}{dx} \psi_{i'+1/2}(x) \rangle = \sum_l \alpha(l)\, \delta_{i+l,i'}, \quad (45)$$

$$\langle \psi_i(x),\ \frac{d}{dx}\varphi_{i'+1/2}(x)\rangle = \sum_l \beta(l)\,\delta_{i+l,i'}, \tag{46}$$

$$\langle \varphi_i(x),\ \frac{d}{dx}\psi_{i'+1/2}(x)\rangle = \sum_l \Gamma(l)\,\delta_{i+l,i'}. \tag{47}$$

By embedding wavelets, the calculation of the integrals (52) to (54) are required as following:

$$\alpha(l) = \int_{-\infty}^{+\infty} \psi(x+l)\,\frac{d}{dx}\psi(x-\frac{1}{2})\,dx, \tag{48}$$

$$\beta(l) = \int_{-\infty}^{+\infty} \psi(x+l)\,\frac{d}{dx}\varphi(x-\frac{1}{2})\,dx, \tag{49}$$

$$\Gamma(l) = \int_{-\infty}^{+\infty} \varphi(x+l)\,\frac{d}{dx}\psi(x-\frac{1}{2})\,dx. \tag{50}$$

Using (21), (22), (25), (26), (29), (42) to (47) we obtain the scalar equations related to H_x corresponding to Maxwell's curl equation (7):

$$\begin{aligned}
&\frac{1}{\Delta t}\ (B^{\varphi x}_{i,j+1/2,k+1/2,n} - B^{\varphi x}_{i,j+1/2,k+1/2,n-1}) \\
&= \sum_l r(l)\left(\frac{E^{\varphi y}_{i,j+1/2,k+l+1,n-1/2}}{\Delta z}\right. \\
&\quad \left. - \frac{E^{\varphi z}_{i,j+l+1,k+1/2,n-1/2}}{\Delta y}\right) \\
&\quad + \sum_l \Gamma(l)\,\frac{E^{\psi y}_{i,j+1/2,k+l+1,n-1/2}}{\Delta z},
\end{aligned} \tag{51}$$

$$\begin{aligned}
&\frac{1}{\Delta t}(B^{\psi x}_{i,j+1/2,k+1/2,n} - B^{\psi x}_{i,j+1/2,k+1/2,n-1}) \\
&= \sum_l \alpha(l)\,\frac{E^{\psi y}_{i,j+1/2,k+l+1,n-1/2}}{\Delta z} \\
&\quad + \sum_l \beta(l)\,\frac{E^{\varphi y}_{i,j+1/2,k+l+1,n-1/2}}{\Delta z} \\
&\quad - \sum_l r(l)\,\frac{E^{\psi z}_{i,j+l+1,k+1/2,n-1/2}}{\Delta y}.
\end{aligned} \tag{52}$$

Other equations of electromagnetic field are obtained straightforwardly by the similar way.

In the inhomogeneous media, constitutive equations such as $\vec{B} = \mu\vec{H}$, $\vec{D} = \varepsilon\vec{E}$ have to be used to obtain electromagnetic field intensities from these flux density functions. This leads to the integral equations or material operators and burdens the additional complexity and storage for the related matrices. In order to reduce the computational burden, space- and time-adaptive grids must be embedded by means of the thresholding procedure.

References

[1] M. Krumpholz and L. P. B. Katehi, "MRTD : New time-domain schemes based on multiresolution analysis," *IEEE Trans. Microwave Theory Tech.*, vol. 44, pp. 555-571, Apr., 1996.

[2] K. S. Yee, "Numerical solution of initial boundary value problems involving Maxwell's equations in isotropic media," *IEEE Trans. Antennas Propagat.*, vol. AP-14, pp. 302-307, May, 1966.

[3] M. Krumpholz, H. G. Winful, and L. P. B. Katehi, "Nonlinear time-domain modeling by multiresolution time domain," *IEEE Trans. Microwave Theory Tech.*, vol. 45, pp. 385-393, Mar., 1997.

[4] M. Werthen and I. Wolff, "A novel wavelet based time domain simulation approach," *IEEE Microwave Guided Wave Lett.*, vol. 6, pp. 438-440, Dec., 1996.

[5] G. Beylkin, "On the representation of operators in bases of compactly supported wavelets," *SIAM J. Numer. Anal.*, vol. 6, pp. 1716-1740, 1992.

[6] W. Sweldens and R. Piessens, "Wavelet sampling techniques," *Proc. the Statistical*

Computing Section, American Statistical Association, pp. 20-29, 1993.

[7] S. G. Mallat, "Multiresolution approximations and wavelet orthonormal bases of $L^2(R)$," *Trans. Amer. Math. Soc.*, vol. 315, pp. 69-87, Sep., 1989.

[8] R. D. Patton and P. C. Marks, "One dimensional finite elements based on the Daubechies family of wavelets," *AIAA J.*, vol. 34, pp. 1696-1698, Aug., 1996.

[9] E. M. Tentzeris, R. L. Robertson, and L. P. B. Katehi, "Space- and time-adaptive gridding using MRTD technique," *IEEE MTT-S International Microwave Symposium Digest*, pp. 337-340, 1997.

[10] I. Daubechies, *Ten lectures on wavelets*, CBMS-NSF Series in Applied Mathematics, SIAM, pp. 167-213, 1992

[11] A. Taflove and M. E. Brodwin, "Numerical solution of steady-state electromagnetic scattering problems using time-dependent Maxwell's equations," *IEEE Trans. Microwave Theory Tech.*, vol. MTT-23, pp. 623-630, Aug., 1975

[12] A. Taflove et al., *Advances in Computational electrodynamics (The finite-difference time-domain method)*, Artech House, pp. 111-162, 1998.

정 영 욱

1997년 2월: 광운대학교 전자공학과(공학사)
1999년 2월: 광운대학교 대학원 전자공학과(공학석사)
1994년 3월~현재: 에이스테크놀로지 통신기술연구소 연구원
[주 관심분야] 웨이브릿, 수치 해석

이 용 민

1993년 2월: 광운대학교 전자공학과(공학사)
1995년 2월: 광운대학교 대학원 전자공학과(공학석사)
1999년 2월: 광운대학교 대학원 전자공학과(공학박사)
1999년 6월~현재: 한국과학기술연구원(KIST) 복합기능세라믹연구센터 위촉선임연구원
[주 관심분야] 마이크로파 및 밀리미터파 능동/수동 회로설계, 이동통신 및 위성통신 부품개발, 전파전파 및 전자기 해석

최 진 일

1992년 2월: 경기대학교 전자공학과(공학사)
1994년 2월: 광운대학교 전자공학과 대학원(공학석사)
1994년 3월~현재: 광운대학교 전자공학과 대학원 박사학위과정
[주 관심분야] 이동통신 및 위성통신 부품개발, 초고주파 부품수치해석

나 극 환

1973년 2월: 연세대학교 전자공학과(공학사)
1977년 2월: 연세대학교 전자공학과 대학원(공학석사)
1981년 7월: 불란서 ENSEEIHT 국립종합공과대학 전자공학과(공학박사)
1981년~현재: 광운대학교 전자공학과 교수
[주 관심분야] 초고주파 회로설계, 레이다 및 위성통신

강 준 길

1979년 2월: 연세대학교 대학원 전자공학과(공학박사)
1980년 8월~1981년 8월: 미국 MIT 객원교수
1992년 3월~1994년 8월: 광운대학교공과대학 학장
1994년 8월~1997년 7월: 광운대학교 총장
1997년 4월~현재: 한국산업인력관리공단 이사
[주 관심분야] 초고주파 응용 및 통신, Video Processing, 산업전자

신 철 재

1964년: 연세대학교 전자공학과(공학사)
1968년: 연세대학교 전자공학과(공학석사)
1983년: 연세대학교 전자공학과(공학박사)
1970년~1977년: 광운대학교 조교수
1986년~1987년: 플로리다대학교 방문교수
1977년~현재: 아주대학교 전기전자공학부 교수
[주 관심분야] 안테나 설계 및 해석, EMI/EMC, 초고주파통신 부품 개발, 전파전파